

Sam F. Iacobellis* and Richard C. J. Somerville

Scripps Institution of Oceanography, University of California, San Diego

1. INTRODUCTION

The formation of precipitation within clouds is affected by many microphysical processes. In liquid water clouds, precipitation is initiated by the coalescence of cloud droplets into larger drop sizes and is generally referred to as the auto-conversion process. Once the larger drop sizes are formed other processes such as accretion and collection can have a significant impact on the precipitation budget. Thus, for a realistic representation of precipitation it is important that the auto-conversion process be accurately parameterized in atmospheric general circulation models (GCMs).

Most modern GCMs now include prognostic cloud parameterizations that treat cloud fraction and cloud water/ice amount as interactive variables. These cloud water/ice amounts are used to prognostically calculate the cloud optical properties that can have a large influence on the model's radiation budget. Thus, the accurate parameterization of precipitation formation, including the auto-conversion process, is important for both modeling of precipitation rates and specification of cloud optical properties (Liu and Daum, 2004; Rotstayn 2000).

In this paper we first compare some model results derived with different parameterizations of precipitation formation in liquid water clouds. We then show additional SCM results found using a more physically realistic ice precipitation formation scheme. The results are analyzed to examine how these more physically complex parameterizations affect the ice water concentration and also what effect, if any, this may have on the cloud liquid water concentration and surface precipitation. This preprint focuses on results from a SCM. At the meeting we will show preliminary results from three-dimensional atmospheric model(s).

2. MODEL

The SCM is an isolated column of atmosphere extending upwards from, and including, the underlying surface. The SCM utilizes 53 layers and thus has a relatively high vertical resolution in comparison to most GCMs. The horizontal extent of the SCM domain is approximately 200 x 250 km and represents the Cloud and Radiation Testbed (CART) at the ARM SGP site. This SCM was used by Iacobellis et al (2003) and is related closely to the "Scripps SCM" that participated in the SCM comparison studies of Ghan et al (2000) and Xie et al (2002).

The control version of the SCM contains the Rapid Radiation Transfer Model (RRTM) longwave radiation transfer scheme described by Mlawer et al (1997) and the CCM3 shortwave radiation parameterization (Briegleb, 1992). The convection scheme is the CCM3 mass flux parameterization (Zhang and McFarlane, 1995; and Hack, 1994).

Cloud amount and cloud water/ice are prognostic variables and are parameterized using the scheme of Tiedtke (1993). Terms representing the formation of clouds and cloud water/ice due to convection, boundary layer turbulence and stratiform condensation processes are included in this parameterization. Cloud water/ice is removed through evaporation and conversion of cloud droplets and ice to precipitation (details described below). Maximum cloud overlap has been assumed throughout this study.

The shortwave optical properties of clouds are parameterized using the schemes of Slingo (1989) for liquid water clouds and McFarquhar et al (2002) for ice clouds. Ice particle effective radius (R_{eff}) is determined using the parameterization described in McFarquhar (2001), while the effective radius of liquid droplets is calculated following Bower et al (1994).

2.1 Precipitation Formation Schemes

The parameterizations of precipitation formation within stratiform clouds (including clouds forming due to convective detrainment) are described below. The formation of precipitation within convective clouds is determined as part of the cumulus convection scheme and is not altered in this study.

2.1.1 Control

The control version of the SCM utilizes the auto-conversion scheme developed by Sundqvist et al (1989) and later used by Tiedtke (1993). In this scheme the conversion of cloud water to precipitation is parameterized as:

$$G_p = c_0 l_c \left[1 - \exp\left(-\frac{l_c}{l_{crit}}\right) \right]^2, \quad (1)$$

where c_0^{-1} is a characteristic time scale for conversion of cloud droplets into raindrops, l_c is the cloud water content averaged per cloud area (in-cloud value), and l_{crit} represents a typical cloud water content at which the release of precipitation begins to be efficient. The parameters c_0 and l_{crit} are adjusted to take into account coalescence due to precipitation falling through the cloud, the Bergeron-Findeisen process, and ice crystal growth within cirrus clouds. As a

* Corresponding author address: Sam F. Iacobellis, Scripps Institution of Oceanography, La Jolla, CA 92093-0224; e-mail: siacobellis@ucsd.edu.

result, the Sundqvist parameterization attempts to account for multiple bulk microphysical processes with a single equation for both ice and liquid regions. Evaporation of falling rain is included as a separate equation as in Tiedtke (1993) and is based on Kessler's scheme (Kessler 1969).

2.1.2 Experiment: Liquid Regions

Manton and Cotton (1977) proposed a parameterization for the auto-conversion of cloud water to precipitation that is based on the original Kessler (1969) scheme, but includes the effect of the cloud droplet concentration:

$$G_{AU} = f_c I_c H(I_c - I_{cm}), \quad (2)$$

where f_c represents a mean collision frequency of cloud droplets that become rain drops, H is the Heaviside step function, and I_{cm} is a threshold cloud water content below which there is negligible conversion of cloud water to rain. Manton and Cotton (1977) express f_c as

$$f_c = r_c^2 E_c V_c N_c, \quad (3)$$

where r_c is the mean volume radius, E_c is the average collection efficiency, V_c is the terminal velocity of a droplet with radius r_c , and N_c is the mean cloud water droplet concentration. The mean volume radius defined as

$$r_c^3 = (3/4) (I_c / N_c \rho_w), \quad (4)$$

where ρ_w is the density of water. The threshold cloud water content is a function of the mean volume radius such that

$$I_{cm} = (4/3) \rho_w r_{cm}^3 N_c \quad (5)$$

with r_{cm} being the threshold mean droplet radius. Manton and Cotton used values $E_c=0.55$ and $r_{cm}=10$ μ m. Unless otherwise specified, the value of N_c is set to 200 cm^{-3} which is a typical value for continental conditions.

The Manton-Cotton formula given by equation (2) only represents the auto-conversion process and the other important microphysical processes must be included via additional parameterizations. In the case of liquid water clouds these processes are accretion (G_{AC}) and collection (G_{CO}) and are parameterized following Rotstayn (1997):

$$G_{AC} = \frac{E_{AC} f R_f I_c}{2 f} \quad (6)$$

$$G_{CO} = 0.24 f_r E_{CO} (R_f^l)^{0.75} I_c \quad (7)$$

where E_{AC} and E_{CO} are mean collection efficiencies, R_f is the frozen precipitation rate falling into the layer, ρ_f is the bulk density of the falling ice, f_r is the fraction of the grid box where rain is occurring, R_f^l is the local

or in-cloud rainfall rate, and f is a slope factor in the size distribution of the falling ice that is parameterized as a function of temperature. The generation of liquid precipitation is simply the sum of the three terms in equations (2), (6), and (7):

$$G_{p.liq} = G_{AU} + G_{AC} + G_{CO} \quad (8)$$

The evaporation of falling rain is included using the formula given by Rotstayn (1997).

2.1.3 Experiment: Ice Regions

The generation of precipitation in ice regions follows from Rotstayn (1997) where all forms of atmospheric ice are represented by a single variable. Unlike rain, falling ice is not assumed to leave the atmosphere during the current timestep. Thus, falling ice entering a grid box from above is treated as a source term for cloud ice. The rate of precipitation of cloud ice is modeled as:

$$G_{p.ice} = \frac{R_f}{z} q_i \frac{\bar{V}_f}{z} \quad (9)$$

where q_i is the mixing ratio of cloud ice water, R_f is the rate at which ice falls into the layer from above minus any sublimation, and V_f is the fall speed of ice. As in Rotstayn (1997), an empirical relation between ice fall speed and cloud ice content based on measurements made by Heymsfield (1977) is used:

$$\bar{V}_f = 3.23 \frac{q_i}{C_i}^{0.17} \quad (10)$$

where C_i is the ice cloud fraction. Equation (9) is integrated analytically which allows some of the ice entering a layer from above to "fall through" and some to remain in the layer. The sublimation of falling ice is parameterized as in Rotstayn (1997).

In the mixed-phase region, the total formation of precipitation from cloud water is simply a linear combination of the liquid and ice components using the fraction of ice (f_{ice}):

$$G_p = (1 - f_{ice}) G_{p.liq} + f_{ice} G_{p.ice} \quad (11)$$

where f_{ice} is the fraction of cloud water that is ice,

$$\begin{aligned} f_{ice} &= 0.0 & T &< 0C \\ f_{ice} &= T/16 & 0C &> T > 16C \\ f_{ice} &= 1.0 & T &> 16C \end{aligned} \quad (12)$$

2.2 Forcing Data

In this study, the SCM is forced with time-dependent horizontal advective fluxes of heat, moisture and momentum from the European Centre for Medium-Range Weather Forecasting (ECMWF) that are

supplied specially for the ARM Program sites (ECMWF, 2002). The surface temperature and surface heat fluxes were also specified from the ECMWF data.

A series of SCM runs were performed, with the starting time of each run spaced 6 hours apart. Each individual SCM run is 36 hours in length, the first 12 hours being a spin-up period where the model temperature and humidity are specified from the ECMWF analysis. The spin-up period is used to allow the SCM cloud variables to reach a *quasi* steady state. After the spin-up period, the SCM temperature and humidity are no longer constrained. Only the last 24 hours of each SCM run is used in the analysis.

The SCM results from all runs are averaged together, thus the model values at any given time are a mean from 4 runs. The staggering of SCM start times by 6 hours (rather than say 24 hours) is to insure that the time of day at start up does not influence the results. Additionally, this method also insures that the results at a given time of day are not always at the end (or beginning) of the model run.

3. OBSERVATIONAL DATA

3.1 Liquid Water Path

3.1.1 Microwave Radiometers

Measurements of liquid water path (*LWP*) were obtained from data collected by five surface-based Microwave Radiometers (MWR) located within the ARM SGP site. The MWR instrument measures the microwave emissions of liquid water molecules at a frequency of 31.4 GHz from which the *LWP* is calculated. At one of the five sites (which is co-located with the cloud radar measurements described below) laser ceilometer measurements are utilized to provide an improved estimate of the mean radiating temperature (Han and Westwater, 1995). The presence of precipitation causes unrealistic values in the retrieved *LWP* (Sheppard, 1996), so time periods in which precipitation occurred are flagged. Precipitating periods are defined as when the MWR brightness temperature exceeds the prescribed maximum and/or if condensation exists on the instrument window as noted in Morris (2005).

Since the *LWP* values would tend to be highest during precipitation periods, the long-term averages from the MWR instrument calculated here may underestimate the actual value of *LWP*. To help alleviate this potential underestimation the *LWP* during precipitation periods is estimated using interpolation between nearest non-precipitating measurements before and after the time period in question. The uncertainty of the *LWP* measurements varies with atmospheric conditions, but is generally on the order of 30 g m⁻² (Marchand et al, 2003).

3.1.1 GOES-8

Estimates of *LWP* were also obtained using the GOES-8 VISST cloud optical thickness data with the approximate relation:

$$= \frac{3}{2} \frac{LWP}{w r_c}, \quad (13)$$

where r_e is the cloud droplet effective radius and is set to 10 microns. The cloud optical thickness includes both liquid and ice clouds, so one may expect this satellite derived *LWP* to overestimate the actual value whereas the *LWP* derived from the surface based MWR data may be an underestimate. In the results presented later in section 4, both observational estimates of *LWP* are used to evaluate the realism of the SCM results.

3.2 LWC and Cloud Frequency Profiles

Liquid water content data at the SGP site is derived from Millimeter Cloud Radar (MMCR) and MWR data together with a relationship relating radar reflectivity to water content. The MMCR data is obtained from the Active Remotely-Sensed Cloud Locations (ARSCL) product available from the ARM data archive (www.arm.gov/data/). The MMCR operates at the SGP Central Facility and produces data with a temporal resolution of 10 seconds and vertical resolution of 45 meters.

For each time record, the radar reflectivity is used to compute cloud water content via the formula of Sassen and Liao (1994) for liquid and Liu and Illingworth (2000) for ice:

$$LWC = \left(\frac{N_c}{3.6} Z \right)^{1.0/1.8} \quad (14)$$

$$IWC = 0.097Z^{0.59} \quad (15)$$

where Z is the radar reflectivity in mm⁶/m³, N_c is the cloud droplet concentration (cm⁻³), and *LWC* and *IWC* are in g m⁻³. Sassen and Liao (1996) found best agreement with empirical research using a value of $N_c=100$ cm⁻³. We note that this value differs from the value of N_c used in the SCM.

At each radar height level, the observed temperature and Eq. (12) are used to determine the whether the cloud is liquid, ice or a mixture of both. Note that this is different from the alternative approach that uses the temperature to separate the *reflectivity* into a liquid and ice component. Here, we use the temperature to separate the *total cloud water* into liquid and ice components. The present approach entails an additional iterative procedure to determine total cloud water that when divided into the liquid and ice fractions produces a total reflectivity using (14) and (15) that matches the reflectivity measured by the MMCR.

For each radar retrieval, the liquid water path (LWP_{rad}) is computed using the values of *LWC* obtained from (14). The *LWC* values are then scaled using the scaling factor, $f=LWP_{mwr}/LWP_{rad}$, where LWP_{mwr} is the liquid water path obtained the MWR

instrument that is co-located with the MMCR instrument. Thus the shape of the LWC profile is determined by the radar measurements, while MWR measurements specify the magnitude of the values.

The ARSCL product also contains a vertical profile of cloud occurrence for each radar retrieval. In the cloud profile results presented in section 4, the base height of the lowest cloud layer was estimated using multipulse lidar measurements which minimizes the effect of larger hydrometeors and helps eliminate false cloud signals due to falling precipitation.

4. RESULTS

In the discussion that follows, SCM results representing a grid box mean are compared to data from the MMCR that represents a point measurement. Both the SCM and MMCR data are time-averaged over a period of at least 24 hours. This helps to some extent in making a comparison between point measurements and grid-mean values, however it should still be kept in mind that there may be discrepancies between the two types of data.

4.1 Liquid Precipitation Formation

The SCM was initially run using the control parameterization for precipitation formation in both liquid and ice regions (SCM-CON). A second run of the SCM was made using the experiment parameterization of precipitation formation in the liquid region (SCM-EXL) and the control scheme used in the ice regions.

4.1.1 27-hour Period During March 2000 SGP IOP

A recent paper by Xu et al (2004) found that single-column models (SCMs) using a Sundqvist type auto-conversion parameterization drastically underestimated the cloud liquid water content during a 27-hour study period within the March 2000 Atmospheric Radiation Measurement (ARM) Program's Intensive Operation Period (IOP) at the Southern Great Plains (SGP) site. Their results also suggest that models using the Manton-Cotton auto-conversion scheme performed much better during this time period.

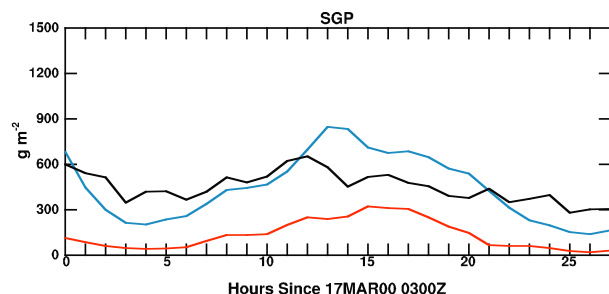


Figure 1. Time evolution of LWP from SCM-CON (red), SCM-EXL (blue) and MWR measurements (black) during the 27-hour period 0300Z March 17 to 0600Z March 18.

The evolution of the column liquid water path from model runs SCM-CON and SCM-EXL during this 27-hour period (0300Z March 17 to 0600Z March 18) is

shown in Figure 1 together with the observed value computed by averaging measurements from the 5 individual MWR locations within the SGP site. Throughout this period run SCM-EXL produces significantly larger values of LWP than run SCM-CON. The LWP results from SCM-EXL are also much closer to the measured values from the MWR data during much of the 27-hour period.

The vertical profiles of cloud fraction and cloud liquid water content (grid-mean and in-cloud values) are shown in Figure 2 from both SCM runs and from MMCR derived measurements. The magnitude of LWC from SCM-EXL is much closer to the MMCR data than the results from SCM-CON, however the shape of the LWC profile from either run does not compare well with the MMCR measurements. This is true for both the grid-mean and in-cloud values. Additionally, the maximum cloud fraction from both SCM runs is about 1 km higher than the MMCR data indicates. While vertically displaced, the maximum cloud fraction from SCM-EXL is closer to the measured cloud fraction maximum compared to the results from SCM-CON.

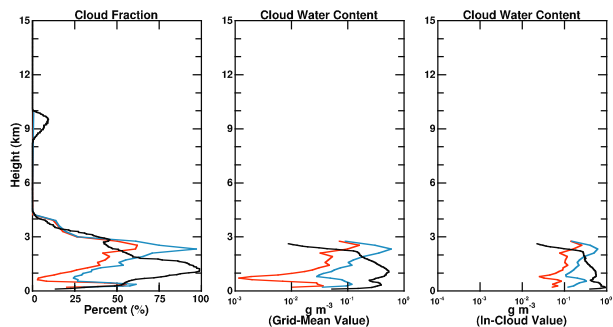


Figure 2. Mean vertical profiles of cloud fraction, grid-mean LWC and in-cloud LWC from run SCM-CON (red), SCM-EXL (blue), and MMCR derived measurements (black) during the 27-hour period 0300Z March 17 to 0600Z March 18.

4.1.2 Monthly and Seasonal Timescales

The 27-hour period examined above was selected in Xu et al (2004) due to the shallow frontal cloud systems observed at the SGP during this time. However, the results from the SCM runs during this period may not be representative of other time periods. In this section, SCM results are examined on monthly and seasonal timescales.

The evolution of the daily mean column liquid water paths from SCM-CON and SCM-EXL were examined along with observational estimates for each month in the year 2000 (daily means from March 2000 are shown in Figure 3). It is evident from this data that the results from the 27-hour period discussed above are not representative of other time periods. The LWP results from model run SCM-CON are in much closer agreement with the MWR measurements than the results from SCM-EXL which tend to significantly overestimate the LWP. This overestimation of the LWP in SCM-EXL is clearly seen when the monthly means are plotted (Figure 4).

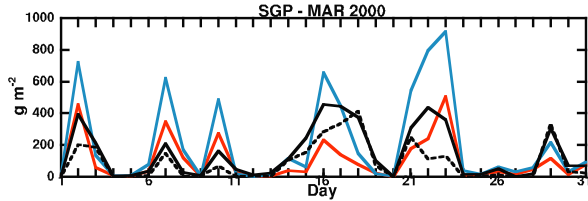


Figure 3. Time series of the daily mean LWP from SCM-C (red), SCM-EXL (blue), MWR measurements (black), and inferred from GOES-8 optical thickness measurements (dashed black) during March 2000.

The mean vertical profiles of cloud fraction and liquid water content averaged on seasonal timescales from both the SCM runs and MMCR measurements are shown in Figure 5. Here we examine the months of November to March to exclude most active convective periods. The SCM runs reproduce the general shape and magnitude of the measured cloud fraction profile. However, the cloud radar measurements indicate a relative cloud maximum in the lowest 2 km, that the SCM results either underestimate or miss altogether.

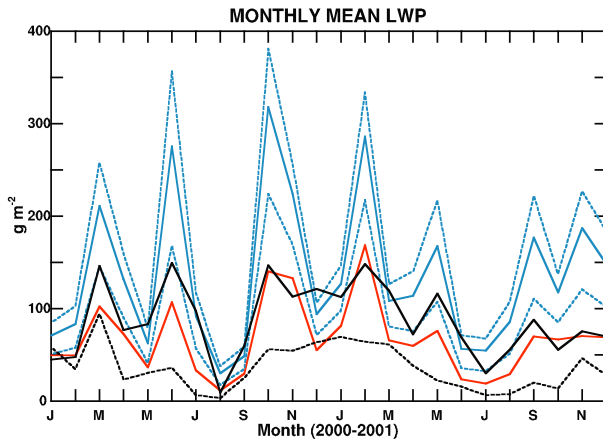


Figure 4. Monthly mean LWP from SCM-CON (red), SCM-EXL (blue), and MWR measurements (black) during 2000-2001. The dashed blue curves are from runs of SCM-EXL using values of $N_c = 100 \text{ cm}^{-3}$ (lower curve) and 300 cm^{-3} (upper curve) while the solid blue curve is from the default run with $N_c = 200 \text{ cm}^{-3}$.

The differences in cloud water content between the two SCM runs are more pronounced than the cloud fraction differences. Model run SCM-EXL consistently overestimates the liquid water content compared to the MMCR measurements. Model run SCM-CON produces a mean cloud water content that is closer in magnitude to the MMCR measurements. However, the shape of the SCM-CON profile generally underestimates the LWC in the lowest 2-3 km and overestimates the LWC above the 3 km level. Part of this is probably related to the SCM not reproducing the low cloud maximum seen in the MMCR cloud fraction data. Another possible cause are errors in the MMCR retrieval due to the presence of both liquid and ice water in the region above 3 km. A linear relationship based on temperature was used in the retrieval algorithm (and the SCM) to separate liquid

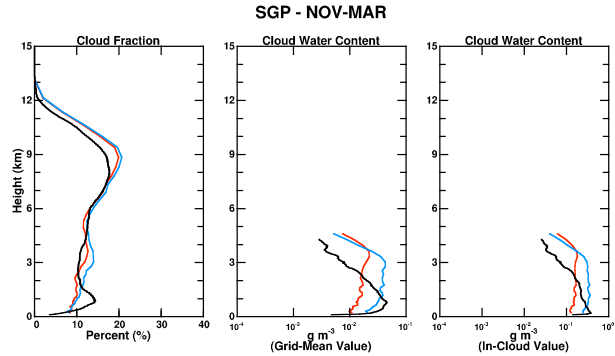


Figure 5. Mean vertical profiles of cloud fraction, grid-mean LWC, and in-cloud LWC from SCM-CON (red), SCM-EXL (blue), and MMCR derived measurements (black) during the months November - March.

water from ice. Since the radar reflectivity is vastly different for ice particles and liquid water droplets, an error in the partitioning of the mixed phases could lead to significant errors in the retrieved amounts of liquid and ice water contents.

The 27-hour time-span examined in section 4.1.1 was a period of shallow frontal clouds at the SGP site. To isolate those times when shallow cloud layers are present at the SGP, we now only include those times when there are shallow clouds present in both the SCM and measured cloud data. Here, shallow is defined as between the surface and 3 km, with no overlying clouds of thickness greater than 1000 m. The results from SCM-EXL compare much better to the measured values of LWC when only these instances of shallow clouds are retained. As in Fig. 5, the shape of the SCM profiles does not agree with the measured profiles, but the overall magnitude is much better simulated by run SCM-EXL.

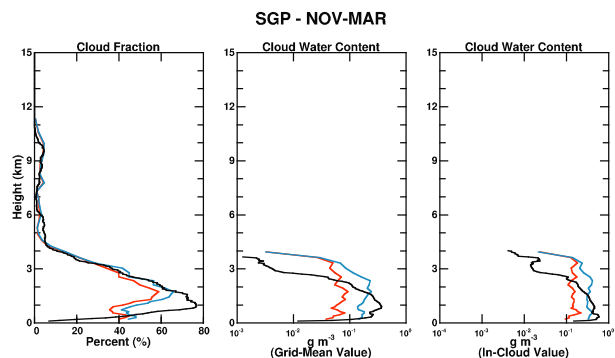


Figure 6. Seasonal mean vertical profiles of cloud fraction, grid-mean LWC, and in-cloud LWC from SCM-CON (red), SCM-EXL (blue), and MMCR derived measurements (black) during the months of November - March. Only those times when shallow clouds are present with no overlying clouds are included in the averages

Figure 7 contains the mean profiles of cloud fraction and liquid water content for those periods in which there were both shallow clouds and higher clouds present in both the SCM and measured cloud data. Here the liquid water content profiles from SCM-CON are much closer to the observed values than the profiles from SCM-EXL. This suggests that the presence of high clouds above the shallow clouds

may have some influence on the modeled and/or observed cloud water content profiles. This possibility is discussed further in section 5.

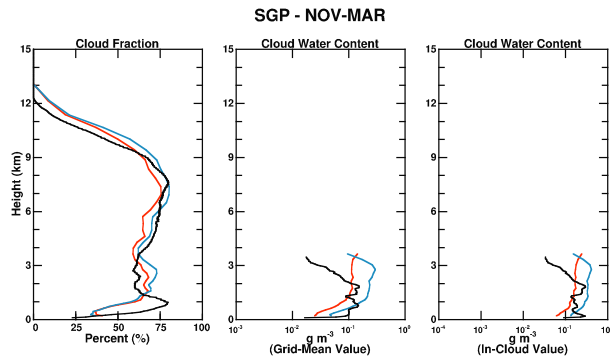


Figure 7. Seasonal mean vertical profiles of cloud fraction, grid-mean LWC, and in-cloud LWC from SCM-CON (red), SCM-EXL (blue), and MMCR derived measurements (black) during the months of November - March. Only those times when shallow clouds and higher clouds are present are included in the averages.

As discussed earlier some uncertainty exists in the MWR LWP retrievals during precipitating periods. The LWP values are used to scale the LWC retrievals from the MMCR instrument. Figure 8 contains the mean profiles of cloud fraction and liquid cloud water content when only those periods where both the SCM and observations indicated no precipitation. Grid-mean LWC values from SCM-EXL compare well to the MWR retrievals, but this is most likely due to the corresponding underestimation of cloud fraction by the model. The in-cloud values of LWC from SCM-CON are clearly much closer to the MWR measurements compared to the results from SCM-EXL.

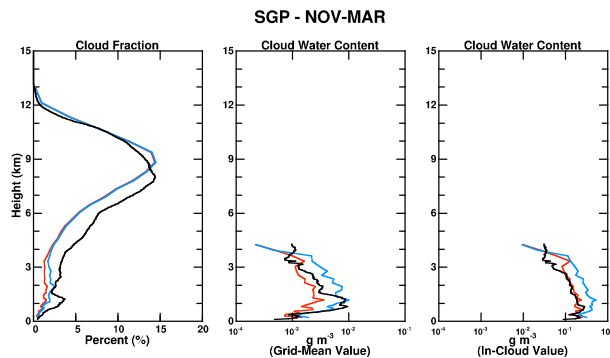


Figure 8. Seasonal mean vertical profiles of cloud fraction, grid-mean LWC, and in-cloud LWC from SCM-S (red), SCM-MC (blue), and MMCR derived measurements (black) during the months of November - March. Only those times when there was no modeled or observed precipitation are included in the averages (no modeled precipitation is defined as less than 1 mm day^{-1}).

4.2 Ice Precipitation Formation

A third run of the SCM was performed using the experiment parameterization of precipitation formation in both the liquid and ice regions (SCM-EXI). The formation of liquid and ice precipitation in SCM-EXI is determined by separate parameterizations and the ice fraction of total cloud water is no longer forced by equation (12) (note: equation (12) is still used to

determine the fraction of liquid and ice cloud water when clouds are formed). Thus, once a cloud forms the relative amount of liquid and ice cloud water is determined by physically based parameterizations rather than a prescribed linear fit to temperature. The impact that the changes in SCM-EXI have on the cloud fraction and cloud water contents is examined below.

Figure 9 shows the mean profiles of cloud fraction and total cloud water content (ice+liquid) during the months of November-March for SCM-CON and SCM-EXI along with MMCR derived measurements. The new ice precipitation physics in SCM-EXI significantly increases the cloud fraction above the 3 km level. As in Fig. 8, only those periods where both the SCM and observations indicated no precipitation were included. Between 3 and 8 km, the results from SCM-EXI agree much better with the MMCR measurements compared to SCM-CON. However, above 8 km SCM-EXI produces too much cloudiness. Both SCM-CON and SCM-EXI produce a cloud fraction maximum that is about 1-2 km higher than that suggested by observations.

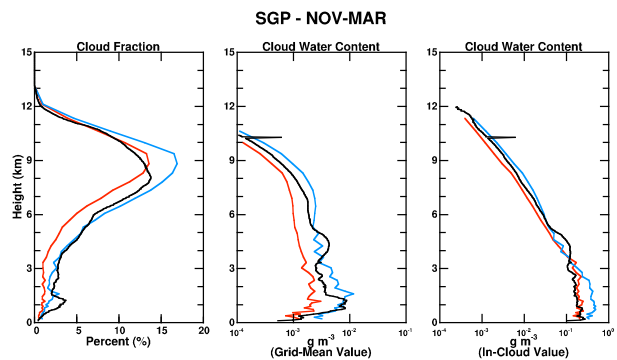


Figure 9. Seasonal mean vertical profiles of cloud fraction and total (ice + liquid) water content (grid-mean and in-cloud values) from SCM-CON (red), SCM-EXI (blue), and MMCR derived measurements (black) during the months of November - March 2000-2001. Only those times when there was no modeled or observed precipitation are included in the averages (no modeled precipitation is defined as less than 1 mm day^{-1}).

Comparison of Figures 8 and 9 indicate that the inclusion of more physically based cloud ice microphysics in run SCM-EXI does not have a large effect on the cloud liquid water profiles (for the period November to March, cloud liquid water extends from the surface to approximately 3 km). However, the cloud ice water profile from run SCM-EXI is closer to MMCR-derived measurements than the results from SCM-CON.

The daily mean precipitation from runs SCM-CON, SCM-EXL, SCM-EXI are shown in Figure 10 together with ARM surface observations for the month of March 2000. Surprisingly, the daily mean precipitation from runs SCM-CON and SCM-EXL are nearly identical while run SCM-EXI generally produces reduced amounts.

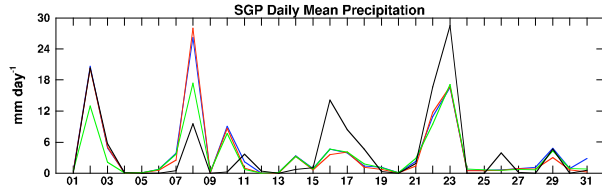


Figure 10. Daily mean precipitation from runs SCM-CON (blue), SCM-EXL (red), SCM-EXI (green), and ARM surface observations (black) during March 2000.

5. CONCLUSIONS

- During the 27-hour period examined by Xu et al (2004), SCM results using the Manton-Cotton auto-conversion parameterizations are more realistic than those results from SCM runs using a Sundqvist type auto-conversion.
- However, over longer time periods the SCM performs better when the Sundqvist auto-conversion scheme is used.
- Analysis indicates that the Manton-Cotton parameterization is more realistic during those periods characterized by shallow low clouds without overlying high clouds.
- SCM results using the Manton-Cotton scheme are particularly sensitive to the specification of the cloud droplet concentration, N_c .
- Inclusion of more physically-based ice precipitation physics results in improved cloud ice concentrations and mid-tropospheric cloud fraction amounts. However, cloud liquid water amounts show little sensitivity.
- Future work will explore whether the presence of high clouds has a significant effect on the precipitation efficiency within underlying lower clouds.

7. ACKNOWLEDGMENTS

This research was supported in part by the Office of Science (BER), U. S. Department of Energy under Grant DOE-FG02-97-ER62338 and the National Oceanic and Atmospheric Administration under Grant NA77RJ0453.

8. REFERENCES

- Bower, K. N., T. W. Chouarton, J. Latham, J. Nelson, M. B. Baker, and J. Jenson, 1994: A parameterization of warm clouds for use in atmospheric general circulation models. *J. Atmos. Sci.*, **51**, 2722-2732.
- Briegleb, B. P., 1992: Delta-Eddington approximation for solar radiation in the NCAR Community Climate Model. *J. Geophys. Res.*, **97**, 7603-7612.
- ECMWF, 2002: The ECMWF operational analysis and forecasting system: The full evolution http://www.ecmwf.int/products/data/operational_system/index.html
- Ghan, S., and co-authors, 2000: A comparison of single column model simulations of summertime midlatitude continental convection. *J. Geophys. Res.*, **105**, 2091-2124.
- Hack, J. J., 1994: Parameterization of moist convection in the National Center for Atmospheric Research community climate model (CCM2). *J. Geophys. Res.*, **99**, 5551-5568.
- Han, Y., and E. R. Westwater, 1995: Remote sensing of tropospheric water vapor and cloud liquid water by integrated ground-based sensors. *J. Atmos. Oceanic Technol.*, **12**, 1050-1059.
- Heymsfield, A. J., 1977: Precipitation development in stratiform ice clouds: A microphysical and dynamical study. *J. Atmos. Sci.*, **34**, 367-381.
- Iacobellis, S. F., G. M. McFarquhar, D. L. Mitchell, and R. C. J. Somerville, 2003: The sensitivity of radiative fluxes to parameterized cloud microphysics. *J. Climate*, **16**, 2979-2996.
- Kessler, E., 1969: *On the Distribution and Continuity of Water Substance in Atmospheric Circulation. Meteor. Monogr.*, **32**, Amer. Meteor. Soc., 84 pp.
- Liu, Y., and P. H. Daum, 2004: Parameterization of the autoconversion process. Part I: Analytical formulation of the Kessler-type parameterizations. *J. Atmos. Sci.*, **61**, 1539-1548.
- Liu, C.-L., and A. J. Illingworth, 2000: Toward more accurate retrievals of ice water content from radar measurements of clouds. *J. Appl. Meteor.*, **39**, 1130-1146.
- Marchand, R., T. Ackerman, E. R. Westwater, S. A. Clough, K. Cady-Pereira, and J. C. Liljegren, 2003: An assessment of microwave absorption models and retrievals of cloud liquid water using clear-sky data. *J. Geophys. Res.*, **108**, 4773, doi:10.1029/2003JD003843.
- Manton, M. J., and W. R. Cotton, 1977: Formulation of approximate equations for modeling moist deep convection on the mesoscale. *Atmos. Sci. Paper, No. 266*, Dept. Atmos. Sci., Colorado State University, Fort Collins, CO.
- McFarquhar, G. M., 2001: Comments on 'Parameterization of effective sizes of cirrus-cloud particles and its verification against observation' by Zhian Sun and Lawrie Rikus (October B, 1999, 125, 3037-3055). *Q. J. R. Meteor. Soc.*, **127**, 261-265.
- McFarquhar, G. M., P. Yang, A. Macke, and A. J. Baran, 2002: A new parameterization of single-scattering solar radiative properties for tropical ice clouds using observed ice crystal size and shape distributions. *J. Atmos. Sci.*, **59**, 2458-2478.
- Mlawer, E. J., S. J. Taubman, P. D. Brown, M. J. Iacono, and S. A. Clough, 1997: Radiative transfer for inhomogeneous atmospheres: RRTM, a validated correlated-k model for the longwave. *J. Geophys. Res.*, **102**, 16663-16682.
- Morris, V., 2005: Microwave radiometer (MWR) handbook. Technical report ARM TR-016, U.S. Department of Energy. (available online at http://www.arm.gov/publications/tech_reports/handbooks/mwr_handbook.pdf)
- Rotstain, L. D., 1997: A physically based scheme for the treatment of stratiform clouds and precipitation in large-scale models. I: Description

- and evaluation of the microphysical processes. *Q. J. R. Meteorol. Soc.*, **123**, 1227-1282.
- Rotstayn, L. D., B. F. Ryan, and J. J. Katzfey, 2000: A scheme for calculation of the liquid fraction in mixed-phase stratiform clouds in large-scale models. *Mon. Wea. Rev.*, **128**, 1070-1088.
- Sassen, K., and L. Liao, 1996: Estimation of cloud content by W-band radar. *J. Appl. Meteor.*, **35**, 932-938.
- Slingo, A., 1989: A GCM parameterization for the shortwave radiative properties of water clouds. *J. Atmos. Sci.*, **46**, 1419-1427.
- Sheppard, B. E., 1996: Effect of rain on ground-based microwave radiometric measurements in the 20-90 GHz range. *J. Atmos. Oceanic Technol.*, **13**, 1139-1151.
- Sundqvist, H., E. Berge, and J. E. Kristjansson, 1989: Condensation and cloud parameterization studies with a mesoscale numerical weather prediction model. *Mon. Wea. Rev.*, **117**, 1641-1657.
- Tiedtke, M., 1993: Representation of clouds in large-scale models. *Mon. Wea. Rev.*, **121**, 3040-3061.
- Xie, S., and co-authors, 2002: Intercomparison and evaluation of cumulus parameterizations under summertime midlatitude continental conditions. *Q. J. R. Meteorol. Soc.*, **128**, 1095-1135.
- Xu, K.-M., and co-authors, 2005: Modeling springtime shallow frontal clouds with cloud-resolving and single-column models. *J. Geophys. Res.*, **110**, D15S04, doi:10.1029/2004JD005153.
- Zhang, G. J., and N. A. McFarlane, 1995: Sensitivity of climate simulations to the parameterization of cumulus convection in the Canadian Climate Centre general circulation model. *Atmos.-Ocean*, **33**, 407-446.